

Risk assessment of reactive local sand use in aggregate mixtures for structural concrete

Kinga Dziedzic^{*}, Michał A. Glinicki

Institute of Fundamental Technological Research, Polish Academy of Sciences, Warsaw, Poland

ARTICLE INFO

Keywords:

Aggregate mixture reactivity
Alkali-silica reaction
Fine aggregate
Kinetic model
Miniature concrete prism test
Slag-blended cement

ABSTRACT

Potential use of marginal fine aggregate in concrete is hindered by prescriptive quality requirements for concrete constituents. Experimental tests were performed on eleven mixtures of coarse and fine aggregates of variable susceptibility to alkali silica reaction (ASR). The miniature concrete prism test was applied for evaluation of ASR-induced expansion and associated changes of elastic properties were evaluated using the resonance modulus testing. Substitution of nonreactive sand with sands of moderate reactivity resulted in a relative increase in concrete expansion by 19–112% and substantial reduction of its elastic properties during the exposure to accelerated ASR environment. The Kolmogorov-Avrami-Mehl-Johnson model, modified to incorporate separately the effects of moderate reactivity of coarse and fine aggregate fractions, successfully described the kinetics of ASR-induced expansion. Beneficial effects of blastfurnace slag used for partial replacement of Portland clinker in blended cements were captured for aggregate combinations.

1. Introduction

The use of local mineral aggregates for construction of infrastructure projects enables materials supply flexibility and reduces backlogs while providing cost efficiency. It is also desirable due to its potential to reduce the environmental burden associated with the massive use of natural aggregate for concrete manufacturing, which can eventually lead to substantial depletion of major mineral deposits. The technical problems and benefits of using marginal fine aggregate in concrete were demonstrated in several experimental and modelling studies, including both manufactured sand, aeolian sand, waste sand or recycled concrete sand [1–5]. Partial replacement of natural river sand by selected manufactured sand or recycled concrete sand was found to provide almost comparable mechanical properties with the reference concrete provided that the replacement is restricted to certain limits. However, concrete durability indicators such as the water absorption, permeability and carbonation rate increase as the replacement ratio of such marginal fine aggregate increases, mostly because of more porous contact zone and more porous matrix, resulting from poor mix workability, inferior grain distribution, inferior bond to cement paste and stress concentration due to flaky-shaped particles [5,6]. That limits the range of feasible applications to mostly non-structural elements or to only non-aggressive environmental conditions.

The selection of aggregate for structural concrete designed for road infrastructure is primarily driven by stringent technical specifications associated with usually expected long-term durability of these outdoor structures. Natural sand, consisting mostly of round and durable mineral particles formed through rock weathering and geological or fluvial transport processes, is highly valued as a component in workable concrete mixtures with predicted high durability performance. Considering rather common exposure of structural elements to environmental aggressions in wet-freeze climate regions, such as freeze-thaw and deicing salt aggression or chloride aggression, the options for selecting alternative aggregate for durable concrete appear to be quite limited. In order to pursue environmental goals, it is crucial to investigate these limitations and develop necessary tools for risk assessment when using marginal aggregate fraction in structural concrete.

One of the key criteria for selecting mineral aggregates for durable structural concrete, as outlined in ASTM C33 [7], is their susceptibility to alkali-silica reaction (ASR). The widely accepted strategy, described in AASHTO R-80 [8], involves evaluating the potential reactivity of aggregates based on their historical field performance, which works well for traditionally used sources of rock aggregate. However, it is important to note that this strategy carries a level of risk due to the challenge of determining whether the aggregate composition remains sufficiently similar to that from previous years. For new quarries or local deposits

^{*} Corresponding author.

E-mail addresses: kdzie@ippt.pan.pl (K. Dziedzic), mglinic@ippt.pan.pl (M.A. Glinicki).

<https://doi.org/10.1016/j.conbuildmat.2023.133826>

Received 7 April 2023; Received in revised form 5 October 2023; Accepted 13 October 2023

Available online 18 October 2023

0950-0618/© 2023 The Authors. Published by Elsevier Ltd. This is an open access article under the CC BY license (<http://creativecommons.org/licenses/by/4.0/>).

without prior performance records, the potential reactivity of aggregate needs to be assessed through petrographic examination and accelerated expansion methods [9], such as those defined in ASTM standards [10–12] or similar RILEM Recommendations or national standards. The quick accelerated mortar bar test [11] has been used to assess potential reactivity of some eco-friendly fine aggregate, such as completely decomposed granite soil [13] or fine recycled aggregate [14]. However, the effects of marginal fine aggregate used along with coarse aggregate on ASR expansive behavior of concrete were not studied in detail. Due to the significant limitations of traditional concrete prism test (CPT) methods [15], RILEM has developed a series of new test procedures to counteract the alkali leaching phenomena by increasing the cross section of concrete prisms [16] or using wrapped prisms [17]. In spite of the recent improvements, the concrete prism test needs to be run for 1 year, preferably 2 years, at 38 °C for meaningful evaluation of aggregate reactivity and ASR mitigation efficiency. The challenge lies in the fact that the time frame available for road infrastructure construction projects is often insufficient for evaluating local aggregate deposits using the concrete prism test.

A recently introduced miniature prism test method (MCPT) [18], based on extensive research by P.R. Rangaraju and co-workers [19,20], is a quicker alternative to the traditional concrete prism test, providing aggregate evaluation results within a maximum of 12 weeks (Table 1). Its suitability for ASR potential recognition was verified for a number of reactive aggregate types, mostly from North-America, with advantageous correlation with field block performance, outperforming the traditional concrete prism test. However, it should be noted that the correlation with field block performance included only few highly reactive aggregates [21] and there is no data available for moderate or late reactive aggregates. The observed expansions of MCPT specimens containing highly reactive coarse aggregate and very-highly reactive fine aggregate demonstrated a close correlation with the relative extent of cracking [22]. The MCPT procedure involves testing either the coarse or fine aggregate fraction (with one of them being nonreactive while the other is being evaluated), thus it has not been used to evaluate the effect of sand reactivity on the reactivity of the aggregate mixture. The objective of this investigation is to determine the ASR performance of inferior aggregate mixtures with different cement combinations in concrete subjected to the MCPT test procedure at 60 °C in a 1 M NaOH solution. The range of investigation covers selected crushed and local

mineral aggregates that exhibit either doubtful (borderline) reactivity or slow-reactivity.

2. Description of the experimental studies

2.1. Materials and specimens

Three coarse crushed aggregates from solid rock were selected for the testing program: trachybasalt (M), amphibolite (A) and greywacke (G), fractions 2/8 and 8/16, intended for use in concrete in according to PN-EN 12620 [23]. Three local quartz sands (B, W, T), and natural sand of volcanic origin (I) were used as fine aggregate, the with maximum grain size of 2 mm. In addition, a mixture of quartz sands (W and B) in a 1:1 wt ratio (designated as X) was included for testing. Table 2 provides the characteristics of the selected aggregates, along with the expansion data determined according to AMBT procedure [11]. The choice of fine aggregate was guided by the variation in potential alkaline reactivity, as reflected by AMBT expansion values ranging from 0.09 % (non-reactive sand) to 0.36 % (reactive sand).

Natural siliceous sand B is obtained from natural sand deposits in northeastern Poland and consists mostly of quartz and feldspar. Natural siliceous sand W is extracted from a riverbed in central Poland and consists of quartz grains, with a substantial content of chert. Natural siliceous sand T consists mainly of quartzite fragments, along with sandstone (up to 20 %) and granite (1 %). It is mined from natural sand deposits in southeastern Poland. Volcanic sand (I) is sourced in southeastern Iceland and contains primarily fragments of basalt, gabbro, granophyre and diabase. The petrographic description of selected fine and coarse aggregates is provided in [24,25]. The reactive minerals detected in fine aggregate consisted of micro- and cryptocrystalline quartz, strained quartz and volcanic glass.

The selected cements for the study include Portland cement CEM I 52.5 R (designated as C1), with an alkali content of $\text{Na}_2\text{O}_{\text{eq}} = 0.88 \%$, and cements blended with granulated blastfurnace slag CEM II/B-S 42.5 R (C2) and CEM III/A 42.5 N (C3) with an alkali content of 0.64 % and 0.49 %, respectively. The chemical composition of the cements is shown in Table 3.

The concrete mixtures were designed following the requirements of the MCPT procedure [18], with a maximum aggregate grain size of 12.5 mm. A total of 15 concrete mixtures were prepared, consisting of 11 mixtures with Portland cement and 4 mixtures with cements blended with ground granulated blastfurnace slag. The missing 2–4 mm fraction of fine aggregate was supplemented with the same fraction of coarse aggregate. The cement content was kept constant at 420 kg/m³, and the water-cement ratio was maintained at 0.45. Sodium hydroxide was added to the mix water to raise the alkali content to $\text{Na}_2\text{O}_{\text{eq}} = 1.25 \%$. The aggregate content in the concrete mix was determined using dry-rodded-density. A deviation from the original standard procedure was the use of a mixture of aggregate fractions with varying potential for

Table 1
Basic features of MCPT method according to AASHTO T 380.

Procedure	AMBT [11]	CPT [12]	MCPT [18]
Aggregate gradation	from 0.150 to 4.75 mm (single fraction) ¹	up to 22.0 mm (fine + coarse) ²	up to 12.5 mm (fine + coarse) ³
Cement content	~585 kg/m ³	420 ± 10 kg/m ³	420 kg/m ³
w/c ratio	0.47	0.42–0.45	0.45
Alkali boosting	none	up to 5.25 kg/m ³ Na ₂ O _{eq}	up to 5.25 kg/m ³ Na ₂ O _{eq}
Specimen size	25x25x285 mm	75x75x285 mm	50x50x285 mm
Exposure conditions	1 M NaOH, 80 °C	RH > 95 %, 38 °C	1 M NaOH, 60 °C
Upper expansion limits ⁴	NR: 0.10 % at 2 weeks MR: 0.30 % at 2 weeks HR: 0.45 % at 2 weeks	NR: 0.04 % at 52 weeks MR: 0.12 % at 52 weeks HR: 0.24 % at 52 weeks	NR: 0.03 % ⁵ at 8 weeks SR: 0.04 % at 8 weeks MR: 0.12 % at 8 weeks HR: 0.24 % at 8 weeks

¹ subjected to crushing, sieving.

² one fraction - nonreactive while the other being evaluated.

³ coarse aggregate subjected to sieving to eliminate particles > 12.5 mm.

⁴ NR-non-reactive, MR – moderately reactive, HR- highly reactive, SR – low/slow reactive.

⁵ or 0.04 % if the expansion rate from 8 to 12 weeks ≤ 0.010 % per 2 weeks.

Table 2
Characteristics of aggregates.

ID	Description	Density [g/cm ³]	AMBT expansion [%]		
			14 days	28 days	
M	coarse	Crushed trachybasalt	2.70	0.188	0.287
A		Crushed amphibolite	2.89	0.159	0.260
G		Crushed greywacke	2.71	0.310	0.523
B	fine	Natural fossil sand	2.65	0.091	0.230
W		Natural river sand	2.66	0.298	0.455
T		Natural fossil sand	2.65	0.357	0.568
I		Natural volcanic sand	2.66	0.320	0.414
X		Mixed sand (50 % B + 50 % W)	2.66*	0.163	0.324

* calculated average value.

Table 3
Chemical composition of cements determined according to PN-EN 196-2 [26].

ID	Cement	Constituent [%]									
		SiO ₂	Al ₂ O ₃	Fe ₂ O ₃	CaO	MgO	SO ₃	Na ₂ O	K ₂ O	LOI	Na ₂ O _{eq}
C1	CEM I 52.5 R	19.42	5.45	2.94	64.10	1.75	3.50	0.24	0.97	1.03	0.88
C2	CEM II/B-S 42.5 R	25.96	5.71	2.37	57.42	2.99	2.72	0.23	0.64	1.09	0.64
C3	CEM III/A 42.5 N	31.00	6.00	1.91	54.09	4.58	2.47	0.27	0.35	1.11	0.49

expansion due to ASR, as indicated in Table 2.

Prismatic specimens with dimensions of 50x50x285 mm, with attached steel studs were cast and compacted using a vibrating table. The manufactured specimens comprised of two sets: the first - intended for the storage in accelerated ASR environment at elevated temperature, the second - intended for water storage at the standard laboratory temperature (reference specimens). After initial storage in molds under high humidity conditions (RH > 95 %) for 24 h, the specimens were immersed in water at 60 °C for 24 h. At the age of two days the initial specimen length was determined. Then the specimens of the first set were immersed in a sodium hydroxide solution at 60 °C and the reference specimens were stored in water at 20 °C. Periodically the specimens were removed from the temperature controlled cabinets to be subjected to nondestructive measurements and returned to the containers for further storage.

2.2. Test methods

Following the standard MCPT procedure (Table 1) the expansion of concrete specimens was measured periodically until the storage time in 1 M NaOH solution at 60 °C reached 12 weeks. The length measurements were taken using a dedicated expansion rig with a digital extensometer of 1 μm accuracy. In addition to expansion measurements, the elastic modulus of concrete was determined using the standard test method for fundamental transverse frequency of concrete specimens as per ASTM C 215 [27]. The resonant frequency of flexural vibrations of prismatic specimens was determined using a GrindoSonic MK5 device with a piezoelectric detector capable of measuring frequency within the range of 40 Hz to 100 kHz, with an accuracy of about 0.005 %. Based on the measured fundamental resonance frequency in flexure, along with the mass and dimensions of the specimen, the resonant elastic modulus of concrete was determined. Simultaneously the reference concrete specimens were stored in water for the same period of time and subjected to resonance modulus testing. Finally, the compressive strength of concrete was measured using a modified standard procedure on 50 mm cubic specimens cut from the concrete prisms after the storage termination. Compressive strength measurements were carried out using a Controls model 50-C46Z00 testing machine, at a loading rate of 2400 N/s.

It should be noted that measurements of the resonant elastic modulus of concrete are not included in the standard MCPT procedure. ASTM C215 [27] test method is intended primarily for detecting changes in the dynamic modulus of elasticity of test specimens that are undergoing exposure to weathering or other types of potentially deteriorating influences. The resonance frequency has basically no relation to the type of potentially damaging phenomena in concrete. However, it has been successfully used to monitor the progress of crack development in concrete and adopted in ASTM C666 as a measure of frost durability. A decrease of elastic modulus by up to 50 % was reported by Mielich [28] in ASR-damaged highway pavements. A degradation trend of the elastic modulus seems to be a good indicator of the internal damage caused by ASR, [29]. Although the crack system in concrete induced by ASR and freeze–thaw cycles could be different as indicated by BCA report [30], it is hypothesized that the development of ASR-induced damage in concrete specimens might be reflected by changes in the resonant modulus of elasticity.

After the resonance modulus testing the prismatic specimens were

used to prepare flat impregnated sections for microscopic observations. The selected prisms were dried at 30 °C for 72 h and vacuum impregnated with epoxy resin with fluorescent dye. Concrete slices 30 mm thick were cut perpendicularly from prismatic specimens and polished to obtain a flat and smooth surface, then dried and re-impregnated. Finally, the surface was polished again to remove excess of fluorescent resin, following the procedure described by Litorowicz [31]. The cross section of concrete was examined in UV light using a digital microscope Dino-Lite Edge.

3. Test results

3.1. Expansion of concrete specimens

The graphs (Figs. 1-3) illustrate the change in length of Portland cement concrete specimens during the exposure to accelerated ASR environment. Based on the standard criteria of the MCPT method, the tested coarse aggregates, when combined with non-reactive sand B, can be classified as non-reactive (trachybasalt) and moderately reactive (amphibolite and greywacke).

For all aggregate mixtures tested, a significant influence of the fine aggregate on the final expansion of the concrete specimens was observed. It was noted that the higher the potential reactivity of sand, as determined by the AMBT, the greater the final expansion of the aggregate mixture in MCPT. Volcanic sand had the greatest effect on the expansion of concrete specimens among all fine aggregates used. Substitution of quartz sand (B) by volcanic sand (I) in aggregate mixture resulted in a 6- and 7-fold increase in the expansion of concrete with the amphibolite and trachybasalt coarse aggregate, respectively. The effect of the quartz sand reactivity on the expansion of concrete containing blends of aggregate was also observed. The magnitude of such relative increase in expansion was found to depend mainly on the reactivity of coarse aggregate used. Replacing non-reactive quartz sand (B) with reactive quartz sand (W) led to a 2-fold increase in the expansion of concrete with amphibolite (A) and an approximate 30 % increase in expansion of concrete specimens with greywacke (G). In the case of concrete specimens with trachybasalt (M) coarse aggregate, the potential reactivity of quartz sand had no significant effect on the final expansion of specimens subjected to accelerated ASR environment. No indication of deceleration in the expansion rate of concrete specimens was observed after 56 days or after 84 days of exposure.

Figs. 4 and 5 present the results of testing a mixture of moderately reactive coarse aggregates (amphibolite and greywacke) and reactive quartz sand (W) with different types of cement. It was observed that the use of cement with the addition of granulated blast furnace slag resulted in a reduction in the expansion of concrete specimens across all analyzed aggregate mixtures. With CEM II/B-S (C2) cement, a decrease in expansion of 60 % was recorded for both aggregates, while for CEM III/A (C3) cement a decrease of 90 and 84 % was recorded for mixtures containing amphibolite and greywacke, respectively. In light of the standard procedure, only CEM III/A proved to be an effective inhibitor of the ASR reaction (expansion < 0.020 % after 56 days).

3.2. Modulus of elasticity and compressive strength of concrete

Table 4 and 5 provide a summary of the results for the resonance elastic modulus and compressive strength of concrete specimens after

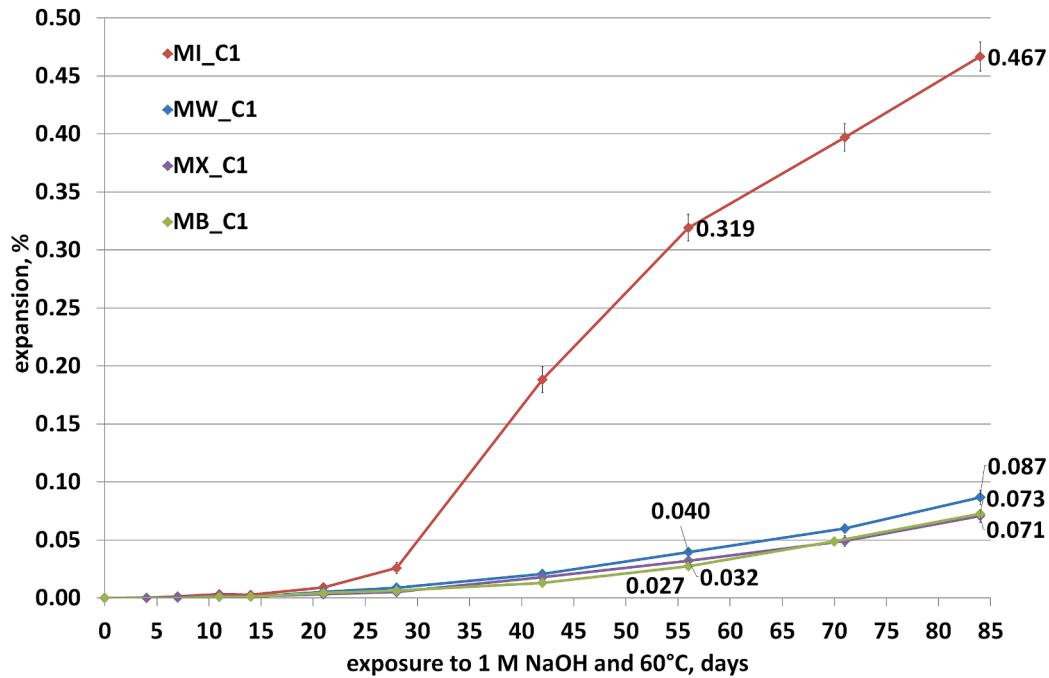


Fig. 1. Expansion of concrete with trachybasalt (M) coarse aggregate and various fine aggregates as a function of exposure time.

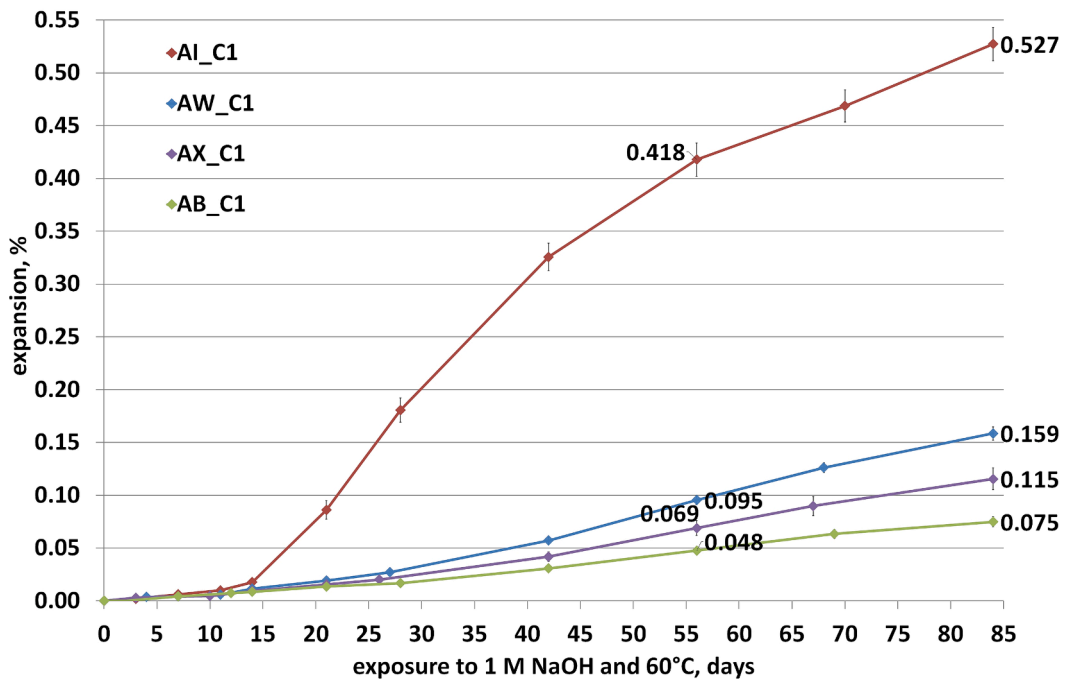


Fig. 2. Expansion of concrete with amphibolite (A) coarse aggregate and various fine aggregates as a function of exposure time.

termination of MCPT expansion tests and after simultaneous water storage at 20 °C (reference concrete specimens). The relative loss is representative for the effects of environmental exposure: mechanical properties resulting from the storage in the conditions of accelerated ASR development are compared with the properties resulting from the standard wet storage of specimens.

A decrease in the elastic modulus of concrete was found due to the exposure to conditions of accelerated ASR development. The specimens

with volcanic sand (AI_C1 and MI_C1) exhibited the greatest decrease in elastic modulus in relation to the reference specimens, up to about 40%. For mixtures containing amphibolite and trachybasalt, the higher the expansion (i.e. more reactive sand in concrete), the greater the decrease in the elastic modulus. However, in the case of graywacke, the reactivity of the quartz sand used had no significant effect on the decrease in elastic modulus - in both mixtures the relative decrease was about 24%. The specimens with slag-blended cements demonstrated the lowest

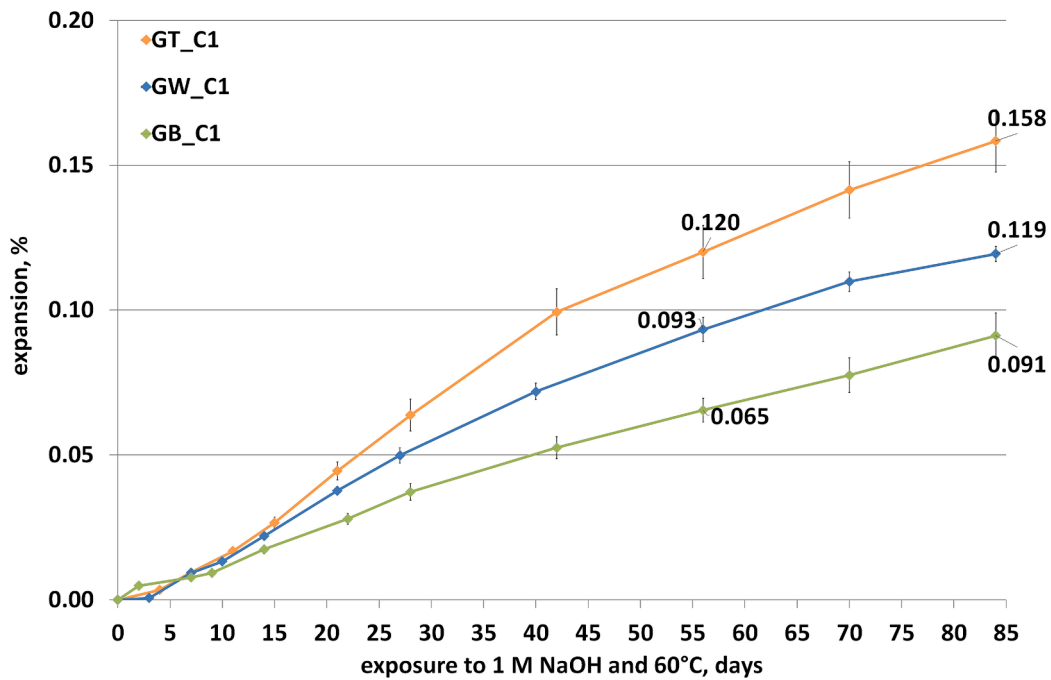


Fig. 3. Expansion of concrete with greywacke coarse aggregate (G) and various fine aggregates as a function of exposure time.

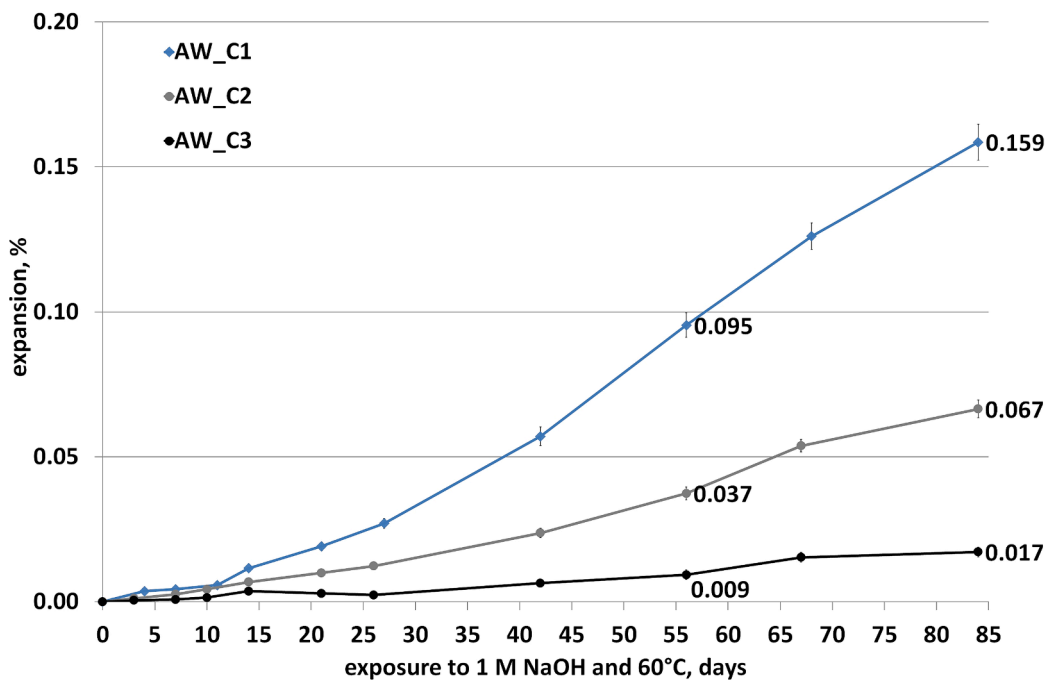


Fig. 4. Expansion of concrete with amphibolite coarse aggregate (A), quartz sand (W) and various cements as a function of exposure time.

decrease in elastic modulus, ranging from 6 to 14 %. Fig. 6 illustrates the correlation between the decrease of resonance elastic modulus and the expansion of all analyzed concrete specimens after 84 days of exposure. A logarithmic correlation with satisfactory fit ($R^2 = 0.91$) was found.

A general view of polished cross-section of concrete specimen after the exposure to accelerated ASR conditions is shown in Fig. 7. The fluorescent epoxy resin that penetrated into the cracks is visualized in UV light, both cracks and voids are displayed. Microscopic images of crack system in similarly exposed specimens are shown in Fig. 8. The cracks are located mostly around aggregate grains and in cement matrix,

some cracks form a connected system. The width of well visible cracks is about 0.10–0.14 mm. Probably some cracks previously filled with ASR products could not be penetrated by the epoxy resin during the impregnated section preparation. No cracks were detected and none visualized in the cross section of reference concrete specimens.

Difficulties in crack identification and quantitative measurements in concrete cross sections are known from Litorowicz [31] and other works. Nevertheless, even a qualitative comparison of the visualized crack system in concrete containing different fine aggregate leads to the observation that more cracking is seen in the specimens with higher

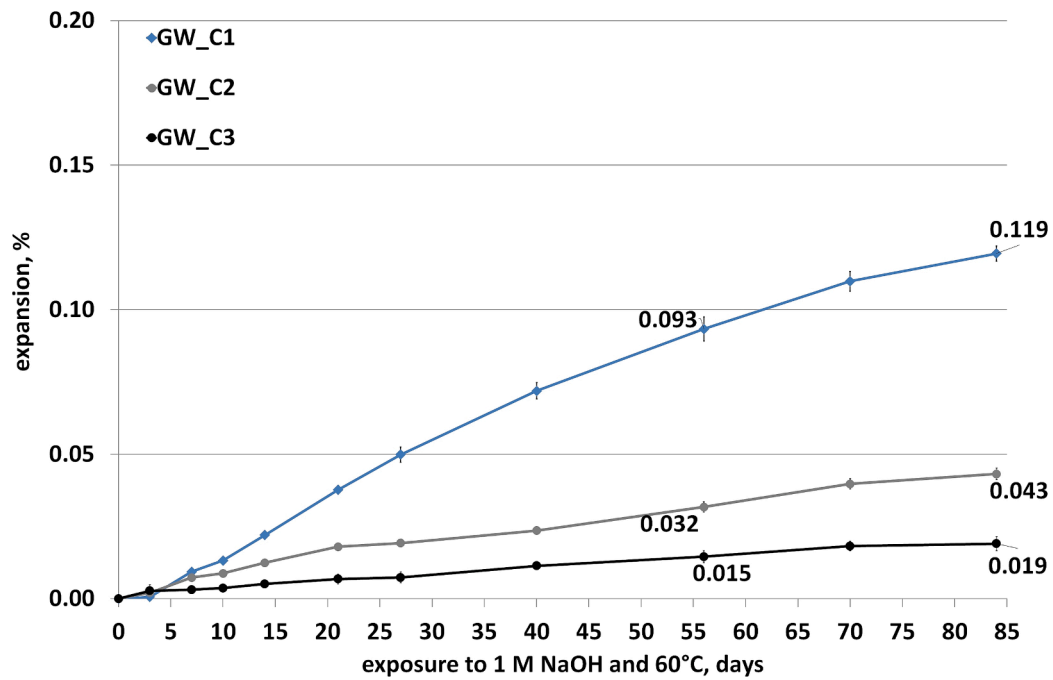


Fig. 5. Expansion of concrete with greywacke coarse aggregate (G), quartz sand (W) and various cements as a function of exposure time.

Table 4

Compressive strength and resonance elastic modulus of concrete specimens with Portland cement CEM I – the influence of aggregate mixtures.

Coarse Aggregate	ID	Compressive Strength [MPa]*			Resonance Elastic Modulus [GPa]**		
		NaOH 60 °C	H ₂ O	Relative loss [%]	NaOH 60 °C	H ₂ O 20 °C	Relative loss [%]
20 °C							
Trachybasalt	MB_C1	66.1 ± 2.7	82.2 ± 3.8	19.6	N/A	N/A	–
	MX_C1	70.5 ± 2.6	76.9 ± 2.6	8.3	40.4	47.0	14.0
	MW_C1	65.6 ± 4.1	77.0 ± 3.5	14.8	38.5	48.5	20.6
Amphibolite	MI_C1	52.2 ± 2.4	81.3 ± 4.8	35.8	29.0	47.8	39.3
	AB_C1	56.6 ± 4.2	67.6 ± 2.3	16.3	44.6	55.7	19.9
	AX_C1	55.5 ± 2.7	63.8 ± 3.1	13.0	43.3	57.8	25.1
Greywacke	AW_C1	51.9 ± 5.7	66.5 ± 1.5	22.0	40.2	58.1	30.9
	AI_C1	46.5 ± 2.9	73.7 ± 4.7	36.9	32.2	54.1	40.5
	GB_C1	60.7 ± 2.7	80.3 ± 2.6	24.4	N/A	N/A	–
	GW_C1	64.3 ± 3.5	73.1 ± 4.8	12.0	37.6	49.5	24.0
	GT_C1	64.2 ± 2.1	73.9 ± 1.9	13.1	38.3	49.9	23.3

N/A – no data due to test device malfunction.

* average value ± standard deviation.

** coefficient of variation from 2.0 % to 4.7 %.

Table 5

Compressive strength and resonance elastic modulus of concrete specimens with amphibolite/greywacke and natural quartz sand W – the influence of blended cement.

Coarse Aggregate	ID	Compressive Strength [MPa]*			Resonance Elastic Modulus [GPa]**		
		NaOH 60 °C	H ₂ O	Relative loss [%]	NaOH 60 °C	H ₂ O	Relative loss [%]
20 °C							
Amphibolite	AW_C1	51.9 ± 5.7	66.5 ± 1.5	22.0	40.2	58.1	30.9
	AW_C2	58.6 ± 3.6	63.5 ± 5.7	7.7	50.8	58.9	13.8
Greywacke	AW_C3	48.2 ± 1.6	60.7 ± 2.4	20.6	50.1	53.5	6.3
	GW_C1	64.3 ± 3.5	73.1 ± 4.8	12.0	37.6	49.5	24.0
	GW_C2	64.7 ± 3.6	63.3 ± 1.7	–2.2	44.5	47.4	6.2
	GW_C3	58.9 ± 2.1	54.6 ± 2.6	–7.9	44.2	48.2	8.3

* average value ± standard deviation.

** coefficient of variation from 0.4 % to 4.4 %.

expansion. For a low expansion specimen (Fig. 8a) cracks in the cement matrix occur locally and do not form a connected crack network. An extensive interconnected system of cracks with particularly prominent

cracks around the aggregate grains is seen for large expansion specimen (Fig. 8c).

Following the guidelines in [31] the digital images were subjected to

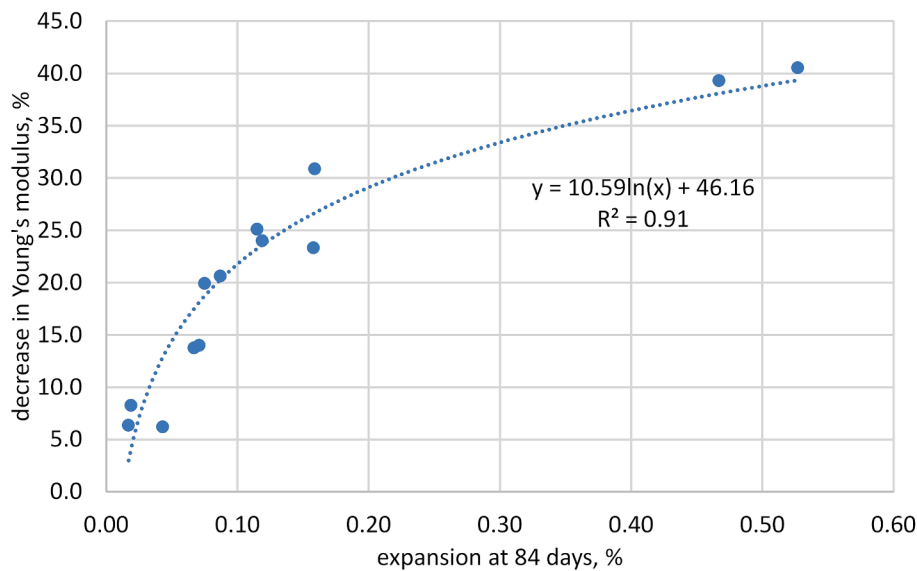


Fig. 6. The relationship between the expansion of specimens and relative reduction of elastic modulus - all concrete mixtures.

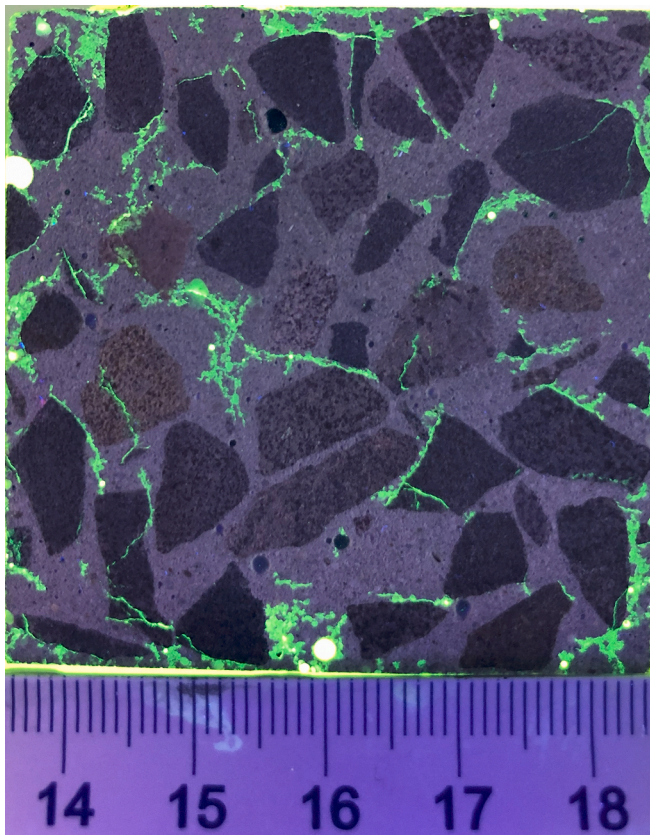


Fig. 7. UV view of the polished impregnated cross section of concrete specimen with trachybasalt aggregate (M) and quartz sand (W) after the exposure to accelerated ASR conditions.

binarization that resulted in the companion images shown in Fig. 8b and 8d. Further image transformation, called skeletonization or thinning, resulted in the crack skeleton of the width of one pixel (not readable for reproduction here). The resulting total length of crack skeleton was digitally measured and the results displayed in this figure provide an estimation of the differences in the observed crack development in concrete. The differences in crack presence and their density (total crack

length per image area) follow the trend of elastic modulus changes: a more developed crack system is observed for specimens characterized by a more pronounced loss of resonance elastic modulus (see Table 4). The crack damage caused by ASR is probably the main reason for the decrease in the elastic modulus of the concrete specimens tested. The development of cracks in concrete is known to cause the dissipation and attenuation of stress waves and a decrease in the fundamental resonant frequency, which is associated with a decrease in elastic modulus (Malone et al., [32]).

The compressive strength of the concrete was also affected by the exposure to conditions of accelerated ASR development. The specimens with volcanic sand (AI_C1 and MI_C1) also showed the greatest decrease in compressive strength, down to about 37 % in relation to the reference concrete. The effect of the origin of the quartz sand, however, was found to be irrelevant. When analyzing the effect of different cements, the specimens with Portland cement exhibited a decrease of 11–12 % in strength, while the concrete with slag-blended cement showed both a decrease (for amphibolite) and a slight increase (for greywacke) in strength compared to the reference specimens.

The preliminary microstructural analysis of concrete, performed using the optical microscopy and scanning electron microscopy with energy-dispersive spectroscopy methods [24,25], revealed the presence of alkali-silica reaction products (Na + and K + ions presence) in cracks in the aggregate grains and in the cement matrix. A more detailed description of the results of microstructural analysis will be presented in a companion paper.

4. Analysis and discussion

4.1. Data analysis with ASR kinetic model

The kinetic relationship, derived using the Kolmogorov-Avrami-Mehl-Johnson (KAMJ) model, was used by Johnston et al., [33,34] to interpret mortar-bar expansion data at 80 °C (AMBT test method). Equation (1) describes the expansion increase over time (t) when using two parameters: k - the expansion constant, which is influenced by the formation and diffusion of the reaction product; M - the Avrami index, which is associated with the form of the reaction product:

$$E_t = 1 + E_{t_0} - \exp[-k(t - t_0)^M] \quad (1)$$

where: E_t - expansion at t day, E_{t_0} - expansion at t_0 day.

Efforts have been made to apply the model to analyze the kinetics of

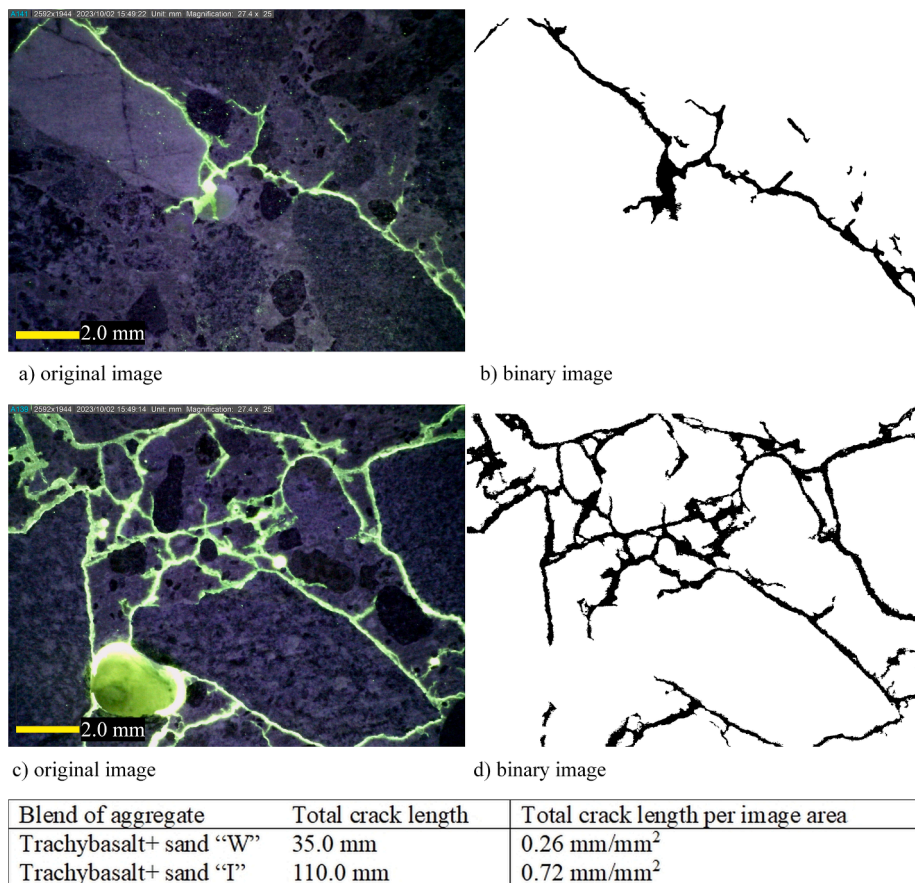


Fig. 8. Crack pattern in the cross section of concrete after the exposure to accelerated ASR conditions: a) + b) trachybasalt aggregate with quartz sand (W), c) + d) trachybasalt aggregate with volcanic sand (I) (the area of each image: 153 mm²).

ASR in concrete under high humidity storage at 38 °C, but the results have been inconclusive thus far. The same approach was employed to the current concrete expansion data obtained in a 1 M NaOH solution at 60 °C. By transforming the model into a linear form Equation (2), in the manner proposed by Johnston [33,34]:

$$Y = M \bullet X + \ln(k) \tag{2}$$

where: $Y = \ln\left(\ln\left(\frac{1}{1+E_0-E_t}\right)\right)$, $X = \ln(t-t_0)$,

it was possible to identify the model parameters. The kinetic model showed a very good fit to the MCPT expansion data, with the coefficient of determination R² ranging from 0.849 to 0.996, but not as strong as the fit to the AMBT expansion data obtained by Islam et al., [35]. Additionally, no clear relationship could be observed between the parameters ln(k) and M and the expansion of concrete specimens. Consequently, the k parameter cannot be used to evaluate the potential reactivity of the aggregate in the same way as in AMBT, because of the greater complexity of the expansion process: contrary to the single finely crushed aggregate system, in MCPT there is a mixture of aggregate fractions with varying reactivity and unknown contribution to the total expansion.

Assuming that the concrete expansion is predominantly determined by the reactivity of coarse aggregate, which constitutes 63 % of the aggregate mix by mass, a modified approach to the parameters identification is proposed. In this approach, the parameter M is considered as a material constant specific to a particular coarse aggregate. Though this approach has its limitations, it effectively highlights the effect of sand reactivity and the impact of mitigating measures on the reaction rate of the aggregate mixture. By comparing the parameter k, a direct comparison of the reaction rate among aggregate mixture can be made.

Table 6

Parameters of the kinetic model for expansion of concrete with Portland cement CEM I – the influence of coarse/fine aggregate mixtures (the fit for 56 days).

Mix ID	Model parameters		Coefficient R ²	ln (k _m)	E ₅₆ [%]	RE ₅₆ [%]
	M _m	k _m				
MB_C1	1.625	0.00004	0.990	-10.1	0.026	6.1
MX_C1	1.625	0.00005	0.984	-9.9	0.030	5.3
MW_C1	1.625	0.00006	0.993	-9.7	0.038	4.8
MI_C1	1.625	0.00057	0.951	-7.5	0.297	7.0
AB_C1	1.445	0.00016	0.991	-8.8	0.048	1.4
AX_C1	1.445	0.00021	0.997	-8.5	0.066	3.5
AW_C1	1.445	0.00030	0.995	-8.1	0.091	4.2
AI_C1	1.445	0.00178	0.990	-6.3	0.426	2.0
GB_C1	1.136	0.00071	0.995	-7.2	0.069	5.1
GW_C1	1.136	0.00116	0.989	-6.8	0.101	8.2
GT_C1	1.136	0.00150	0.993	-6.5	0.128	6.9

Table 6 shows the calculation results for MCPT concrete expansion data with different aggregate mixtures, while Table 7 summarizes the results for different types of cement. A constant M_m parameter is assumed as the average value of M parameters for concrete mixes with a specific coarse aggregate, calculated according to Equation (2). The new k_m parameter was calculated by reducing Equation (1) into the following linear form:

$$Y = k_m \bullet X \tag{3}$$

where: $Y = \ln\left(\frac{1}{1+E_0-E_t}\right)$, $X = (t-t_0)^{M_m}$.

The coefficient of determination R² for the proposed linear regression (Eq. (3) in the analyzed dataset ranges from 0.948 to 0.997. The

Table 7

Parameters of the kinetic model for expansion of concrete with coarse amphibolite or greywacke and quartz sand W – the influence of slag cement (the fit for 56 days).

Mix ID	Model parameters		Coefficient R ²	ln(k _m)	E ₅₆ [%]	RE ₅₆ [%]
	M _m	k _m				
AW_C1	1.445	0.00030	0.995	-8.1	0.091	4.2
AW_C2	1.445	0.00012	0.997	-9.0	0.037	0.0
AW_C3	1.445	0.00003	0.954	-10.4	0.009	1.9
GW_C1	1.136	0.00116	0.989	-6.8	0.101	8.2
GW_C2	1.136	0.00037	0.948	-7.9	0.036	12.0
GW_C3	1.136	0.00013	0.996	-8.9	0.015	2.5

average error of prediction of expansion at 56 days (RE₅₆) predominantly decreased to 8 % or less. For each type of coarse aggregate, when considering the calculated constant M_m, the k_m parameter demonstrates a systematic increase as the expansion in MCPT test increases. In the dataset that includes fine aggregates of varying reactivity (Table 6), it becomes possible to determine the threshold value of ln(k_m) that indicates a detrimental expansion in the MCPT for a given aggregate mixture in concrete: ln(k_m) = -9.5 for the studied set of aggregates.

The dataset on concrete with slag cements, as presented in Table 7, provide the means to evaluate the expansion threshold for effective ASR mitigation. Considering the appropriate expansion limit of 0.02 % at 56 days of MCPT exposure [18], the required ln(k_m) can be predicted for a particular mixture of aggregates. The required relative reduction of ln(k_m) in comparison to the reference value for Portland cement concrete is found as 22 % and 26 % for the “AW” and “GW” mixtures. This corresponds roughly to a minimum slag content of 45 % or 47 % in blended cement.

4.2. Coarse aggregate and aggregate mixture reactivity evaluation

None of the studies [19–21] that present the results of reactivity testing using the MCPT method have specifically analyzed the reactivity of trachybasalt, greywacke or amphibolite. Only diabasalts [20], which are a variety of basalt like trachybasalts, were tested and found to be nonreactive in MCPT and other reactivity test methods, including CPT and AMBT. Aggregates identified as trachybasalts that contained small amounts of volcanic glass were also determined to be nonreactive by the chemical method and AMBT [36]. Silva et al., [37] analyzed four trachybasalts, one of which was petrographically classified as potentially reactive due to its volcanic glass content. Although trachybasalts were found nonreactive using AMBT tests, they turned to be reactive in the 2-year CPT. The potential reactivity of basaltic rocks identified petrographically is subject to significant error due to the high variability of basalt deposits. Accelerated mortar bar test is not recommended to identify the reactivity of magmatic rocks, especially basalts, whereas CPT is recommended to be extended to 2 years. These remarks shed light on the contradictory classification of trachybasalt rock evaluated using AMBT and MCPT methods.

Greywacke rock is commonly considered as an example of a well-recognized reactive aggregate of sedimentary origin [38]. Examples of greywacke from Australia, Canada, the UK, the US and South Africa have shown the presence of reactive forms of silica, i.e., microcrystalline and cryptocrystalline quartz. Amphibolite rock is also described in the literature as an example of a potentially reactive metamorphic aggregate - with the presence of micro and cryptocrystalline quartz. Given this context, the results of the current reactivity evaluation of coarse rock aggregate using MCPT method align with classification of similar rocks in the literature.

The evaluation of aggregate mixture susceptibility to alkali-silica reaction should be assessed on the whole aggregate combination. This is because [9] even a harmless amount of reactive silica in either fine or coarse aggregate alone might be damaging in their combination. As

shown by Sanchez et al., [39], the expansion of concrete containing two sizes of reactive aggregate was not the same as the sum of two single expansions measured using only one size of the aggregate. For such a purpose a performance testing approach is used, usually by means of concrete prism testing at 38 or 60 °C [40]. The role of fine aggregate reactivity was also revealed by Deschenes and Hale [41], who analyzed cases of ASR damage in structures. The river sand, previously considered non-reactive, was found to be the cause of the damage. Combining this sand with crushed granite in concrete specimens resulted in an expansion of 0.039 % after one year of CPT, while combining it with crushed limestone showed nonreactive behavior with an expansion of only 0.025 %. However, other studies [42] have shown that testing at 38 °C may not be suitable for identifying reactive aggregates with slower kinetics, unless the test duration is extended. Therefore, the elevated temperature is suggested to be more adequate for characterization of slow reactive aggregates. The current results at 60 °C obtained using MCPT on such slow or borderline reactive coarse aggregates revealed a clearly increasing expansion of concrete specimens when used in combination with sand fraction of increasing reactivity. The most severe damage occurred when a higher amount of reactive silica was present. That seems to be characteristic for rather low reactivity forms of silica like micro- and cryptocrystalline quartz and strained quartz. Interestingly, similar effects of the reactivity of sand on the ASR performance of aggregate combinations were observed at 60 °C testing with external alkali supply [43,44]. Changing natural quartz sand to crushed limestone sand resulted in a decrease in the expansion of concrete specimens, although the effect of the sand varied depending on the coarse aggregate used and the concentration of the external alkali solution. At present, there is no outdoor exposure site data available to confirm the findings from laboratory testing.

The role of sand denoted as “I” needs to be discussed in more detail, as it differs in origin from the other fine aggregate used. According to [45], sand “I” contains mainly basalt grains, unaltered and altered (tholeiitic basalts), as well as rhyolite and basaltic glass. Its high reactivity was found by [46], both in the laboratory and in outdoor testing of cubes. The current expansion data at 80 °C showed its rather moderate reactivity (Table 2). However, when combined with coarse aggregate it demonstrated an extreme susceptibility to accelerate the rate of expansion in MCPT, much higher than reactive sands containing micro- and cryptocrystalline quartz and deformed quartz. Since there is a reason to believe that sand “I” is releasing alkalis over time [47], this phenomenon might contribute to acceleration of the alkali silica reaction progress. There is no such indication of alkali release for quartz sand “W”. Previous research [48] demonstrated that alkaline feldspars and micas in aggregates can supply a significant amount of alkalis when exposed to alkaline solutions and promote alkali-silica reaction. The alkali release from fine aggregate may accelerate the development of ASR of coarse aggregate, and this effect could be more prominent for coarse aggregate that are more susceptible to ASR (note the difference between expansion of concrete containing amphibolite and trachybasalt). However the considered timeframe is rather short, might be insufficient for a substantial alkalis release. It is also possible that sand “I” is susceptible to the testing temperature and exhibits the pessimum behavior, which could explain the rather moderate expansion in AMBT. Kawabata et al., [49] analyzed ASR of concrete with highly reactive andesite (magmatic rock) at different temperatures and found that the specimens tested at the temperature of 40 °C exhibited the highest final expansion after more than 500 days. To resolve this issue the further tests are needed.

4.3. Effects of ASR on mechanical properties of concrete

The currently obtained test results (Fig. 6) revealed a substantial reduction in the resonance elastic modulus proportional to the final expansion of specimens. The degradation of concrete properties induced by the conditions of accelerated ASR development was also significant in

respect to the compressive strength. As shown in Fig. 9, a correlation is found between the strength reduction and elastic modulus reduction due to the storage in the conditions of ASR enhancement. The results are generally in accordance with the literature data reviewed in [50,51]. The degree of deterioration of mechanical properties is expected to depend on the reactivity of the aggregate, grain size, and ASR gel properties.

Such relationships as in Figs. 6 and 9 are important for enhanced understanding of mechanical effects derived from ASR development in concrete. A relationship between the macroscopic expansion and elastic modulus of concrete is a basis for model description of ASR-gel induced microcracking of concrete [52], assumed to occur in the aggregates or in the cement paste matrix. Due to ASR-gel pressure the pre-existing microcracks can propagate, but the propagation may be also driven by other actions (loads, temperature changes, etc.) if they occur. Following the damage evaluation, the phenomenological damage mechanics approach is used that links changes of elastic modulus with diffused microcrack system development. The prolonged cement hydration and subsequent crack healing can take place in relatively young concrete and in a small extent, so generally the crack propagation in time leads to a cumulative effect, described by the increased crack density.

The effect of ground granulated blast furnace slag in blended cement is illustrated in Fig. 10, showing a close-to linear relationship between the Portland clinker content and ASR-induced expansion of specimens, as well as the corresponding reduction in elastic modulus. As in Fig. 9, the decrease in elastic modulus is strongly correlated with expansion - the greater the expansion, the greater the elastic modulus reduction, which may indicate less damage in concrete (fewer cracks) as a result of ASR mitigation with slag partially replacing Portland clinker in blended cement.

The mechanism of ASR mitigation as a result of the addition of granulated blastfurnace slag is not yet clearly recognized, but several factors have been proposed, including the reduction of available alkali, matrix permeability, and calcium hydroxide content [53]. The higher the slag content, the greater the ability to inhibit the reaction [54], and the minimum amount of slag required to inhibit the reaction depends on the aggregate reactivity and the alkali content in the concrete [55]. The effectiveness of ASR mitigation is also affected by slag fineness, with finer slag generally exhibiting higher effectiveness [56]. In our study, a 60 % decrease in expansion was observed for CEM II/B-S, and up to 90 % for CEM III/A, with only the latter demonstrating effectiveness in

inhibiting the reaction in MCPT. There are no clear guidelines for the granulated blast furnace slag content needed to inhibit the reaction, however it should definitely be higher than that of other SCMs, most often above 50 % [53]. In a study [57], it was shown that changing the slag content from 50 % to 65 % resulted in a twofold increase in the time for concrete samples to reach the same level of expansion. The addition of slag at 50 % by weight of cement has been found to be effective in preventing the reaction, even surpassing cement with low alkali content [58] - after 9 years of exposure at 38 °C and high humidity, samples with slag exhibited an order of magnitude lower expansion compared to reference samples. However, in another study [21] on concrete with highly reactive aggregates, a slag content of 40 % was unable to effectively inhibit the reaction in MCPT and concrete blocks, despite demonstrating effectiveness in CPT.

Our study revealed a decrease in compressive strength as the granulated blast furnace slag content in cement increased for specimens stored in water for 84 days. It has been observed that slag blended cement reduces the early compressive strength of concrete but increases the long-term strength compared to Portland cement [54]. However, the long-term compressive strength of concrete depends on various factors such as w/c, temperature and type of treatment, and slag content [59]. Conflicting observations regarding compressive strength can be found in the literature. In [60], it was noted that compressive strength decreases with increasing slag content and air curing, but with curing in water for 90 days and a content of about 50–60 %, an increase in compressive strength was observed compared to concrete with Portland cement. Conversely, in [61], using a slag content of 50 % and water curing, a lower compressive strength (by about 12 %–17 %) was observed compared to concrete with Portland cement. Regarding the modulus of elasticity, both an increase (by 22 % for 50 % slag [62]) and a decrease in comparison to concrete with Portland cement were observed [60]. Another study [63] found a decrease in the elastic modulus of high-performance concrete with increasing slag content (20, 35, 50 % by weight of cement) - by about 16 % at 50 % slag content. To counteract these drawbacks of using slag as a substitute for Portland cement, the production of blended cement, as per EN 197-1 [64], typically involves separate slag grinding to elevated fineness and that makes factory blended slag-cement more strength efficient with no compromise on ASR mitigation efficiency.

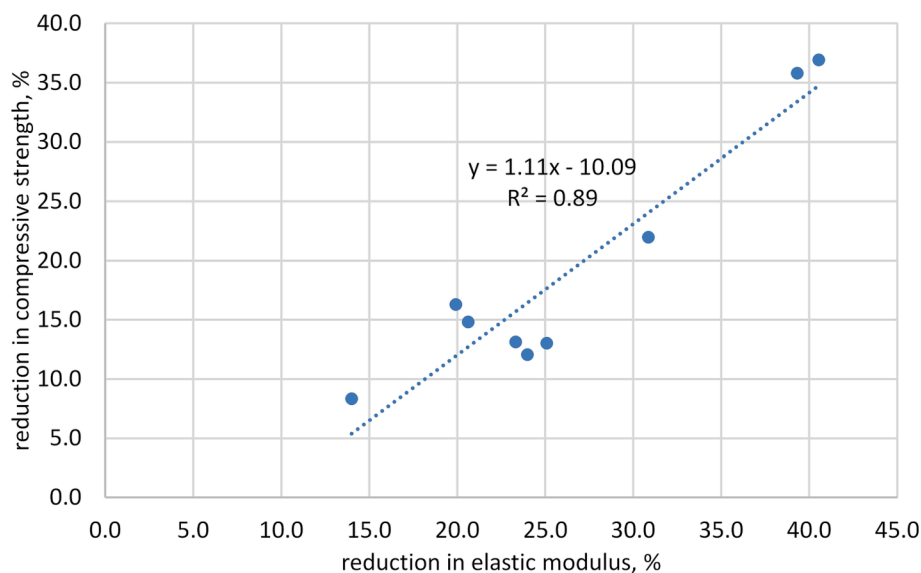


Fig. 9. Correlation between the strength loss and reduction in resonance modulus of concrete after 84 days storage in the conditions of accelerated ASR development - concrete mixtures with Portland cement CEM I.

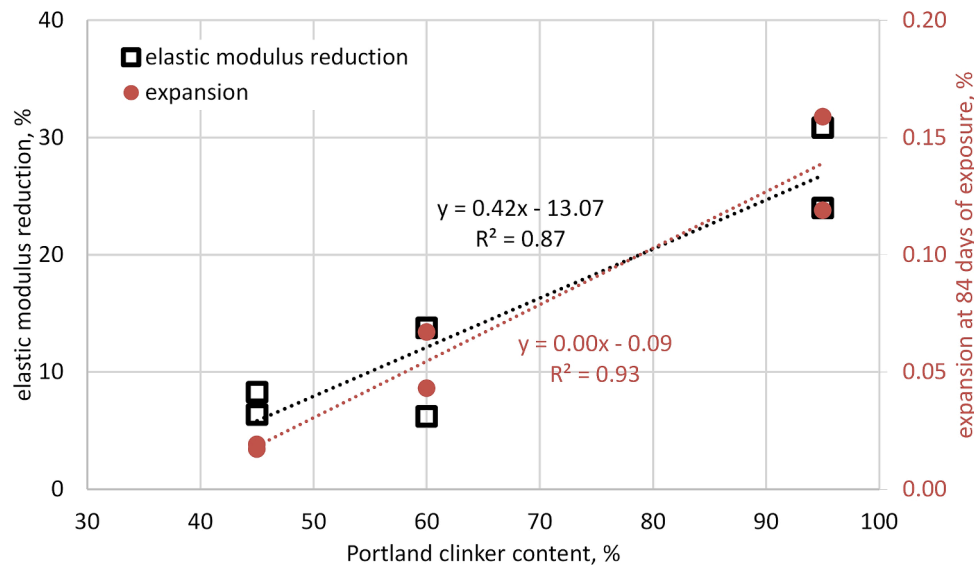


Fig. 10. Effects of Portland clinker content in cement blended with ground granulated blast furnace slag on the ASR-induced expansion of concrete specimens and corresponding resonance elastic modulus reduction measured after 84 days storage in the conditions of accelerated ASR development.

5. Conclusions

Based on the performed experimental investigation, the following conclusions can be drawn.

1. The Miniature Concrete Prism Test is found effective in evaluating the reactivity of aggregate mixtures consisting of fine and coarse aggregates of different origins, containing slowly reacting silica minerals. Due to the presence of moderately reactive quartz sand the expansion of concrete containing mixed aggregates increased by 19–112 % after 84 days, depending on the reactivity level of coarse aggregate.
2. Contrary to AMBT results, the coarse trachybasalt aggregate exhibited nonreactive behavior in MCPT. The amphibolite and greywacke coarse aggregate were confirmed to be moderately reactive.
3. The ASR-induced expansion kinetics were successfully described using the modified KAMJ model, which separately incorporated the effect of reactivity of the coarse and fine aggregate fractions. A threshold value of $\ln(k_m) = -9.5$ was found beyond which a given aggregate mixture exhibited a detrimental expansion in miniature concrete prism tests.
4. A substantial decrease in the resonance elastic modulus of concrete by 6–40 % was observed due to MCPT environmental exposure conditions, logarithmically proportional to the expansion of specimens and linearly related to the clinker content in slag blended cements used.
5. Beneficial effects of blastfurnace slag used for partial replacement of Portland clinker in blended cements CEM II/B-S and CEM III/A were demonstrated for moderately reactive aggregate mixtures. These included a significant reduction of expansion and good stability of elastic properties of concrete in an ASR-promoting environment.

Considering the above statements regarding the suitability of MCPT and its ability to assess the reactivity of concrete within a short time frame, it is believed that the MCPT method is a useful testing tool to support the potential application of local sands for infrastructure construction.

Funding

This research did not receive any specific grant from funding

agencies in the public, commercial, or not-for-profit sectors.

CRedit authorship contribution statement

Kinga Dziejdz: Writing – original draft, Visualization, Methodology, Investigation, Data curation, Conceptualization. **Michał A. Glinicki:** Supervision, Conceptualization, Validation, Writing – review & editing.

Declaration of Competing Interest

The authors declare that they have no known competing financial interests or personal relationships that could have appeared to influence the work reported in this paper.

Data availability

Data will be made available on request.

References

- [1] A. Branavan, C. Konthesingha, A. Nanayakkara, Performance evaluation of cement mortar produced with manufactured sand and offshore sand as alternatives for river sand, *Constr. Build. Mater.* 297 (2021), 123784, <https://doi.org/10.1016/j.conbuildmat.2021.123784>.
- [2] M.N. Akhtar, Z. Ibrahim, N.M. Bunnori, M. Jameel, N. Tarannum, J.N. Akhtar, Performance of sustainable sand concrete at ambient and elevated temperature, *Constr. Build. Mater.* 280 (2021), 122404, <https://doi.org/10.1016/j.conbuildmat.2021.122404>.
- [3] M. Nedeljković, J. Visser, B. Šavija, S. Valcke, E. Schlangen, Use of fine recycled concrete aggregates in concrete: a critical review, *Journal of Building Engineering* 38 (2021), 102196, <https://doi.org/10.1016/j.jobe.2021.102196>.
- [4] Behnood A., Olek J., Glinicki M.A., Predicting compressive strength of recycled concrete aggregate using M5' model, *Brittle Matrix Composites 11 - Proceedings of the 11th International Symposium on Brittle Matrix Composites, BMC -11, IPPT PAN, Warsaw, 2015*, 381-391.
- [5] Z. Yu, L. Wu, C. Zhang, T. Bangi, Influence of eco-friendly fine aggregate on macroscopic properties, microstructure and durability of ultra-high performance concrete: a review, *Journal of Building Engineering* 65 (2023), 105783, <https://doi.org/10.1016/j.jobe.2022.105783>.
- [6] Y. Cao, Y. Wang, Z. Zhang, H. Wang, Recycled sand from sandstone waste: a new source of high-quality fine aggregate, *Resour. Conserv. Recycl.* 179 (2022), 106116, <https://doi.org/10.1016/j.resconrec.2021.106116>.
- [7] ASTM C33/C33M-18, Standard Specification for Concrete Aggregates. ASTM International.
- [8] AASHTO R 80-17, Standard Practice for Determining the Reactivity of Concrete Aggregates and Selecting Appropriate Measures for Preventing Deleterious

- Expansion in New Concrete Construction. American Association of State Highway and Transportation Officials.
- [9] P. Nixon, B. Fournier, Assessment, testing and specification, in: I. Sims, A. Poole (Eds.), *Alkali-Aggregate Reactions in Concrete – A World Review*, CRC Press, 2017, pp. 33–61.
- [10] ASTM C295/C295M-19, Standard Guide for Petrographic Examination of Aggregates for Concrete. ASTM International.
- [11] ASTM C 1260 -21, Standard Test Method for Potential Alkali Reactivity of Aggregates (Mortar-Bar Method). ASTM International.
- [12] ASTM C1293-20, Standard Test Method for Determination of Length Change of Concrete Due to Alkali-Silica Reaction. ASTM International.
- [13] Y. Song, S. Ma, J. Liu, Z.Q. Yue, Laboratory investigation of CDG soil as source of fine aggregates for Portland cement concrete, *Constr. Build. Mater.* 367 (2023), 130226, <https://doi.org/10.1016/j.conbuildmat.2022.130226>.
- [14] A. Barragán-Ramos, C. Ríos-Fresneda, J. Lizarazo-Marriaga, N. Hernández-Romero, Rebar corrosion and ASR durability assessment of fly ash concrete mixes using high contents of fine recycled aggregates, *Constr. Build. Mater.* 349 (2022), 128759, <https://doi.org/10.1016/j.conbuildmat.2022.128759>.
- [15] F. Rajabipour, E. Giannini, C. Dunant, J.H. Ideker, M.D.A. Thomas, Alkali-silica reaction: current understanding of the reaction mechanisms and the knowledge gaps, *Cem. Concr. Res.* 76 (2015) 130–146.
- [16] T.F. Rønning, B.J. Wigum, J. Lindgård, Recommendation of RILEM TC 258-AAA: RILEM AAR-10: determination of binder combinations for non-reactive mix design using concrete prisms–38 °C test method, *Mater. Struct.* 54 (2021) 204, <https://doi.org/10.1617/s11527-021-01679-w>.
- [17] K. Yamada, Y. Kawabata, M.R. de Rooij, et al., Recommendation of RILEM TC 258-AAA: RILEM AAR-13: application of alkali-wrapping for concrete prism testing to assess the expansion potential of alkali-silica reaction, *Mater. Struct.* 54 (2021) 201, <https://doi.org/10.1617/s11527-021-01684-z>.
- [18] AASHTO T 380-2019, Standard Method of Test for Potential Alkali Reactivity of Aggregates and Effectiveness of ASR Mitigation Measures (Miniature Concrete Prism Test, MCPT). American Association of State Highway and Transportation Officials.
- [19] E.R. Latifee, P.R. Rangaraju, Miniature concrete prism test: rapid test method for evaluating alkali-silica reactivity of aggregates, *J. Mater. Civ. Eng.* 27 (2015), [https://doi.org/10.1061/\(ASCE\)MT.1943-5533.0001183](https://doi.org/10.1061/(ASCE)MT.1943-5533.0001183).
- [20] H. Konduru, P.R. Rangaraju, O. Amer, Reliability of miniature concrete prism test in assessing alkali-silica reactivity of moderately reactive aggregates, *Transportation Research Record: Journal of the Transportation Research Board* 2674 (2020) 4, <https://doi.org/10.1177/0361198120912247>.
- [21] J. Tanesi, T. Drimalas, K.S.T. Chopperla, M. Beyene, J.H. Ideker, H. Kim, L. Montanari, A. Ardani, Divergence between performance in the field and laboratory test results for alkali-silica reaction, *Transportation Research Record: Journal of the Transportation Research Board* 2674 (2020) 5, <https://doi.org/10.1177/0361198120913288>.
- [22] K.S.T. Chopperla, T. Drimalas, M. Beyene, J. Tanesi, K. Folliard, A. Ardani, J. H. Ideker, Combining reliable performance testing and binder properties to determine preventive measures for alkali-silica reaction, *Cem. Concr. Res.* 151 (2022), 106641, <https://doi.org/10.1016/j.cemconres.2021.106641>.
- [23] PN-EN 12620: 2010 Aggregates for concrete, Polish Committee for Standardization.
- [24] M.A. Glinicki, D. Józwiak-Niedźwiedzka, A. Antolik, K. Dziedzic, K. Gibas, Susceptibility of selected aggregates from sedimentary rocks to alkali-aggregate reaction, *Roads and Bridges - Drogi i Mosty* 18 (1) (2019) 5–24, <https://doi.org/10.7409/rabdim.019.001>.
- [25] D. Józwiak-Niedźwiedzka, K. Gibas, M.A. Glinicki, Petrographic identification of reactive minerals in domestic aggregates and their classification according to RILEM and ASTM recommendations, *Roads and Bridges - Drogi i Mosty* 16 (3) (2017) 223–239, <https://doi.org/10.7409/rabdim.017.015>.
- [26] PN-EN 196-2: 2013 Method of testing cement Chemical analysis of cement, Polish Committee for Standardization.
- [27] ASTM C215-19 Standard Test Method for Fundamental Transverse, Longitudinal, and Torsional Resonant Frequencies of Concrete Specimens, ASTM International.
- [28] O. Mielich, Alkali-silica reaction (ASR) on German motorways: an overview, *Otto-Graf-Journal* 18 (2019) 197–208.
- [29] C. Lu, S. Bu, Y. Zheng, K. Kosa, Deterioration of concrete mechanical properties and fracture of steel bars caused by alkali-silica reaction: a review, *Structures* 35 (2022) 893–902, <https://doi.org/10.1016/j.istruc.2021.11.051>.
- [30] British Cement Association, *The diagnosis of alkali-silica reaction-Report of a working party*, British Cement Association, Wexham Springs, Slough, U.K., 1992.
- [31] A. Litorowicz, Identification and quantification of cracks in concrete by optical fluorescent microscopy, *Cem. Concr. Res.* 36 (8) (2006) 1508–1515, <https://doi.org/10.1016/j.cemconres.2006.05.011>.
- [32] C. Malone, J. Zhu, J. Hu, A. Snyder, E. Giannini, Evaluation of alkali-silica reaction damage in concrete using linear and nonlinear resonance techniques, *Constr. Build. Mater.* 303 (2021), 124538, <https://doi.org/10.1016/j.conbuildmat.2021.124538>.
- [33] D. Johnston, D. Stokes, R. Surdahl, A kinetic-based method for interpreting ASTM C 1260, *Cement, Concrete and Aggregates* 22 (2) (2000) 142–149, <https://doi.org/10.1520/CCA10474J>.
- [34] Johnston, D., Stokes, D., Fournier, B., Surdahl, R., Kinetic Characteristics of ASTM C1260 Testing and ASR-induced Concrete Damage. 12th International Conference on Alkali-Aggregate Reaction, 2004, Beijing, China.
- [35] M.S. Islam, N. Ghafoori, Evaluation of alkali-silica reactivity using ASR kinetic model, *Constr. Build. Mater.* 45 (2013) 270–274, <https://doi.org/10.1016/j.conbuildmat.2013.03.048>.
- [36] M. Tapan, Alkali-silica reactivity of alkali volcanic rocks, *Eur. J. Environ. Civ. Eng.* 19 (1) (2015) 94–108, <https://doi.org/10.1080/19648189.2014.939303>.
- [37] A.S. Silva, I. Fernandes, D. Soares, J. Custódio, A.B. Ribeiro, Portuguese Experience in ASR Aggregate Assessment, Sao-Paulo, Brazil, 2016.
- [38] I. Fernandes, A.M. Ribeiro, M. Broekmans, I. Sims, *Petrographic atlas: characterisation of aggregates regarding potential reactivity to alkalis, RILEM TC 219-ACS recommended guidance AAR-1.2, for use with the RILEM AAR-1.1 petrographic examination method*, Springer (2016).
- [39] L.F.M. Sanchez, S. Multon, A. Sellier, M. Cyr, B. Fournier, M. Jolin, Comparative study of a chemo-mechanical modeling for alkali silica reaction (ASR) with experimental evidences, *Constr. Build. Mater.* 72 (2014) 301–315, <https://doi.org/10.1016/j.conbuildmat.2014.09.007>.
- [40] Rønning T.F., Lindgård J., Borchers I., ASR performance testing concepts – RILEM AAR-10, AAR-11 and AAR-12, Proceedings of the 16th ICAAR, Lisbon, Portugal.
- [41] R.A. Deschenes, W.M. Hale, Alkali-silica reaction in concrete with previously inert aggregates, *J. Perform. Constr. Facil* 31 (2017) 2, [https://doi.org/10.1061/\(ASCE\)CF.1943-5509.0000946](https://doi.org/10.1061/(ASCE)CF.1943-5509.0000946).
- [42] P.J. Nixon, I. Sims, *RILEM Recommendations for the Prevention of Damage by Alkali-Aggregate Reactions in New Concrete Structures: State-of-the-Art Report of the RILEM Technical Committee 219-ACS*, Springer, 2015.
- [43] Hermerschmidt W., Müller C., Böhm M., Investigations on the influence of sand and testing conditions on the expansion behavior of concretes in ASR tests, Proceedings of the 16th ICAAR, Lisbon, Portugal.
- [44] M.A. Glinicki, K. Bogusz, D. Józwiak-Niedźwiedzka, M. Dąbrowski, ASR performance of concrete at external alkali supply - effects of aggregate mixtures and blended cement, *Int. J. Pavement Eng.* 24 (2023) 1, <https://doi.org/10.1080/10298436.2023.2171038>.
- [45] Wigum B.J., Björnsdóttir V.D., Ólafsson H., Iversen K., Alkali Aggregate Reaction in Iceland - New Test Methods, Report No.: VH 2007-036, 2007.
- [46] Wigum B.J., Assessment and development of performance tests for alkali aggregate reaction in Iceland, In: Drimalas, T., Ideker, JH, Fournier, B (Eds.) 14th International Conference on Alkali-Aggregate Reactions in Concrete, Austin, Texas, USA, pp. 10.
- [47] B.J. Wigum, G.J. Einarsson, *Testing of Icelandic Aggregates and Various Binders – Laboratory Vs. Field: A Decade of Results and Experiences Vol. 1* (2022) 575–586.
- [48] E. Menéndez, R. García-Rovés, B. Aldea, Incidence of alkali release in concrete dams, Evaluation of Alkalies Releasable by Feldspars, MATEC Web of Conferences 199 (2018) 03006, <https://doi.org/10.1051/mateconf/201819903006>.
- [49] Y. Kawabata, C. Dunant, K. Yamada, K. Scrivener, Impact of temperature on expansive behavior of concrete with a highly reactive anhydrite due to the alkali-silica reaction, *Cem. Concr. Res.* 125 (2019), 105888, <https://doi.org/10.1016/j.cemconres.2019.105888>.
- [50] A. Mohammadi, E. Ghiasvand, M. Nili, Relation between mechanical properties of concrete and alkali-silica reaction (ASR); a review, *Constr. Build. Mater.* 258 (2020), 119567, <https://doi.org/10.1016/j.conbuildmat.2020.119567>.
- [51] A. Hafci, L. Turanlı, F. Bektas, Effect of ASR expansion on mechanical properties of concrete, *Cement Wapno Beton* 26 (1) (2021) 12–23, <https://doi.org/10.32047/CWB.2021.26.1.2>.
- [52] T. Iskhakov, J.J. Timothy, G. Meschke, Expansion and deterioration of concrete due to ASR: Micromechanical modeling and analysis, *Cem. Concr. Res.* 115 (2019) 507–518, <https://doi.org/10.1016/j.cemconres.2018.08.001>.
- [53] R.B. Figueira, et al., Alkali-silica reaction in concrete: Mechanisms, mitigation and test methods, *Constr. Build. Mater.* 222 (2019) 903–931, <https://doi.org/10.1016/j.conbuildmat.2019.07.230>.
- [54] ACI-Committee-233, Report on the Use of Slag Cement in Concrete and Mortar (ACI 233R-17), American Concrete Institute, Farmington Hills, MI, 2017.
- [55] M.D.A. Thomas, F.A. Innis, Effect of slag on expansion due to alkali-aggregate reaction in concrete, *ACI Mater. J.* 95 (6) (1998) 716–724.
- [56] Y. Kwon, A study on the alkali-aggregate reaction in high-strength concrete with particular respect to the ground granulated blast-furnace slag effect, *Cem. Concr. Res.* 35 (2005) 1305–1313, <https://doi.org/10.1016/j.cemconres.2004.09.021>.
- [57] A. Bouikni, R.N. Swamy, A. Bali, Durability properties of concrete containing 50% and 65% slag, *Constr. Build. Mater.* 23 (2009) 2836–2845, <https://doi.org/10.1016/j.conbuildmat.2009.02.040>.
- [58] J. Duchesne, M.-A. Berube, Long-term effectiveness of supplementary cementing materials against alkali-silica reaction, *Cem. Concr. Res.* 31 (2001) 1057–1063, [https://doi.org/10.1016/S0008-8846\(01\)00538-5](https://doi.org/10.1016/S0008-8846(01)00538-5).
- [59] E. Özbay, M. Erdemir, H.I. Durmus, Utilization and efficiency of ground granulated blast furnace slag on concrete properties – a review, *Constr. Build. Mater.* 105 (2016) 423–434, <https://doi.org/10.1016/j.conbuildmat.2015.12.153>.
- [60] E. Güneysi, M. Gesoglu, A study on durability properties of high-performance concretes incorporating high replacement levels of slag, *Mater. Struct.* 41 (2008) 479–493, <https://doi.org/10.1617/s11527-007-9260-y>.
- [61] A. Al-Yousuf, T. Pokharel, J. Lee, E. Gad, K. Abdouka, J. Sanjayan, Effect of fly ash and slag on properties of normal and high strength concrete including fracture energy by wedge splitting test: Experimental and numerical investigations, *Constr. Build. Mater.* 271 (2021), 121553, <https://doi.org/10.1016/j.conbuildmat.2020.121553>.

- [62] X. Jin, Z. Li, Effects of mineral admixture on properties of young concrete, *J. Mater. Civ. Eng.* 15 (5) (2003) 435–442, [https://doi.org/10.1061/\(ASCE\)0899-1561\(2003\)15:5\(435\)](https://doi.org/10.1061/(ASCE)0899-1561(2003)15:5(435)).
- [63] D. Shen, Y. Jiao, Y. Gao, S. Zhu, G. Jiang, Influence of ground granulated blast furnace slag on cracking potential of high performance concrete at early age, *Constr. Build. Mater.* 241 (2020), 117839, <https://doi.org/10.1016/j.conbuildmat.2019.117839>.
- [64] PN-EN 197-1: 2012 Cement Part 1: Composition, specifications and conformity criteria for common cements, Polish Committee for Standardization.